Civil and Project Journal, 2027, 8(11), 42-58
https://doi.org/10.22034/cpj.2026.598896.1470

Civil and Project Journal
http://www.cpjournals.com/

Research Article

Numerical Evaluation of EPS Geofoam Inclusion for Lateral Earth Pressure and Displacement Reduction in Retaining Walls

Mahla Faqihi Movahed[1], Bahram Ta'negonbadi[2]*

1- M.Sc. Graduate in Civil Engineering, University of Bojnord, Iran.
2*- Assistant Professor, Department of Civil Engineering, University of Bojnord, Iran.

Received: 24 July 2026; Revised: 29 July 2026; Accepted: 31 August 2026 Published: 21 January 2027

Abstract

The present study numerically investigates the effectiveness of expanded polystyrene (EPS) geofoam inclusions for reducing lateral earth pressure and wall displacement under static drained and undrained conditions. A two-dimensional finite-element model was developed in PLAXIS 2D for a 5 m-high concrete retaining wall supported by layered soil profiles comprising soft clay (CL), soft silt (ML), and loose silty sand (SM). Three EPS unit weights (0.22, 0.29, and 0.39 kN/m³) and four inclusion thicknesses (0.5, 1.0, 1.5, and 2.0 m) were investigated. Soil behavior was represented using the Mohr–Coulomb model, while the wall and EPS were modeled as linear-elastic materials with interface elements for soil–structure interaction. The numerical results were compared with an analytical at-rest earth-pressure reference as a consistency check.

Within the investigated range, EPS-22 (unit weight 0.22 kN/m³) with a thickness of 1.0 m was adopted as a practical reference configuration, reducing lateral earth pressure and maximum wall displacement by approximately 79% and 22%, respectively, for the reference clay–sand profile. Geofoam performance was strongly influenced by soil type, stratification, wall height, and drainage condition. Under undrained conditions, lateral earth-pressure reductions were approximately 22–28%, compared with 50–80% under drained conditions. The results indicate that EPS geofoam can be used as an effective lightweight, compressible inclusion to mitigate static lateral loads on retaining structures. EPS grade and thickness will be selected as appropriate for site conditions and design considerations.

Keywords: *Geofoam, Lateral earth pressure, Retaining wall, Finite-element analysis, Soil–structure interaction, PLAXIS*

Cite this article as Faqihi Movahed,M and Tanegonbadi,B . (2027). Numerical Evaluation of EPS Geofoam Inclusion for Lateral Earth Pressure and Displacement Reduction in Retaining Walls. *Civil and Project journal, 8*(11), 42-58. doi: https://doi.org/10.22034/cpj.2026.598896.1470

ISSN: 2676-511X

Corresponding author E-mail address: b.gonbadi@ub.ac.ir*

Civil and Project Journal, 2027, 8(11), 42-58
https://doi.org/10.22034/cpj.2026.598896.1470

1- Introduction

Common engineering projects such as ports, excavations, railroads, bridges, roads, buildings, and sewer infrastructure use retaining walls to prevent soil collapse, control water ingress, and stabilize the construction system. Retaining walls interact directly with the surrounding foundation soil; therefore, realistic characterization of the ground and lateral earth-pressure response is essential for safe and economical design. The magnitude and distribution of lateral earth pressure depend strongly on wall movement, soil stiffness and strength, and the resulting soil–structure interaction [1]. Recent studies have likewise emphasized the importance of soil–foundation interaction and the reliable characterization of geotechnical stiffness and strength parameters in interpreting deformation response [2,3].

The determination of active and at-rest earth-pressure distributions is therefore a fundamental aspect of retaining-wall design [4]. Classical approaches, including the Rankine and Coulomb theories, provide useful analytical estimates under simplified soil and wall conditions. However, these approaches may not adequately represent complex soil profiles, deformable inclusions, soil–structure interaction, or drainage effects. Consequently, reducing lateral earth pressure through alternative ground-engineering measures has received considerable attention [4].

Soil is generally strong in compression and shear but weak in tension. Reinforcement systems can therefore be introduced to modify soil behavior. In the past, natural materials such as reeds and timber were used to reinforce soil. Currently, the most common materials in the systems are metallic and polymeric materials, such as geosynthetics. Reinforcement based on polymers offers many advantages, including low weight, ease of transportation and installation, low maintenance, and high resistance to environmental degradation [1].

Lightweight, compressible materials can be installed adjacent to the wall of retaining structures to reduce the load transferred from the backfill. Expanded polystyrene (EPS) geofoam is a lightweight, compressible polymeric material used as backfill or as a compressible inclusion behind retaining structures. Previous investigations have examined the effects of EPS thickness, density or grade, wall height, and backfill properties on lateral earth pressure [5–10]. More recent experimental, analytical, and numerical studies have extended this work to short- and long-term response under surcharge loading, semi-empirical prediction of lateral pressure, and limited-surcharge conditions [11–13].

The interfaces between geofoam blocks and adjacent soil or structural materials can represent critical zones under loading. Accordingly, the mechanical properties of EPS and its interfaces are important design considerations. Sheeley [14] conducted direct-shear tests on geofoam–geofoam, geofoam–concrete, and geofoam–geomembrane interfaces and showed that interface resistance depends strongly on the contacting material. Beju and Mandal [15] demonstrated that EPS density is an important index property because compressive strength and elastic modulus generally increase with density. The dependence of EPS stiffness and shear response on material grade has also been documented experimentally [16].

Padade and Mandal [17] performed triaxial tests on EPS geofoam and reported increasing deviatoric resistance with increasing density. Another important aspect is long-term deformation since EPS can creep under sustained stress. Beju and Mandal [18] documented compression-creep behavior, while more recent retaining-wall model tests have shown that time-dependent EPS compression can influence long-term lateral-pressure reduction [11]. These findings indicate that EPS grade should be selected by considering both pressure reduction and allowable short- and long-term deformation.

Previous numerical studies have demonstrated the potential of EPS geofoam to reduce lateral loads on retaining structures [5–13,19–21]; however, comparatively little attention has been paid to its performance in fine-grained and layered soil systems under different drainage conditions. The principal contribution of the present study is a unified parametric evaluation of the combined effects of soil type and stratification, drained versus undrained response, EPS unit weight and thickness, and retaining-wall height on both lateral earth pressure and wall displacement. This integrated framework provides a systematic basis for evaluating how these interacting parameters govern the performance of EPS geofoam as a compressible inclusion.

2- Research Methodology

The two-dimensional finite element analysis was done using PLAXIS 2D. The investigation was organized into four main stages: (i) selection of a baseline soil profile and retaining-wall geometry; (ii) evaluation of different EPS geofoam unit weights and inclusion thicknesses; (iii) sensitivity analyses for soil type, soil stratification, wall height, and drainage condition; and (iv) comparison of the numerical results with an analytical at-rest earth-pressure reference.

The baseline backfill consisted of soft clay (CL). The lateral earth pressure acting on the retaining wall and the resulting wall displacement were obtained from the finite-element analysis. The Mohr–Coulomb constitutive model was adopted for the soils because the objective was a comparative parametric assessment of lateral earth pressure rather than a detailed prediction of nonlinear hardening behavior. The concrete wall and EPS geofoam were represented by linear-elastic constitutive behavior. An interface formulation was used at the soil–wall contact to account for soil–structure interaction.

The study subsequently considered soft silt (ML) and loose silty sand (SM) as alternative soil profiles. Based on the parametric results, EPS-22 (unit weight 0.22 kN/m³; density 21.6 kg/m³) with a thickness of 1.0 m was adopted as a practical reference configuration for the subsequent sensitivity analyses. This selection represents a practical threshold within the investigated range and is not intended as a formal or global optimization. The resulting lateral pressure distributions were also compared with an analytical at-rest earth pressure reference as a numerical consistency check.

3- Materials

3-1- Soil

Soil parameters for numerical modeling were obtained from geotechnical investigation reports prepared by Paidar Sazeh Golestan Co. for residential areas in Gonbad-e Kavus, Golestan Province, northeast of Iran. Three typical soils were considered: soft clay (CL), soft silt (ML), and loose silty sand (SM). CL soil was used as the control material. The principal physical, stiffness, and strength parameters used in the analyses are summarized in Table 1.

Table 1. Properties of the soils used in the numerical analyses

Soil	γ_{dry} (kN/m³)	γ_{wet} (kN/m³)	ν	E (MPa)	Vs (m/s)	w (%)	PL (%)	LL (%)	Strength parameters
CL	13.5	17.1	0.35	5.0	100	27	20	45	c′=9 kPa; φ′=18.5°; cu=17 kPa
ML	14.4	17.8	0.35	5.5	140	24	22	43	c′=5 kPa; φ′=18.2°; cu=19 kPa
SM	16.3	19.3	0.30	9.0	170	18	17	19	c′=2–5 kPa; φ′=24.5°

3-2- EPS Geofoam

The EPS geofoam properties were adopted from Khan and Meguid [20]. Three geofoam types with nominal unit weights of 0.22, 0.29, and 0.39 kN/m³ were considered. Their elastic properties and Poisson's ratios are given in Table 2.

Table 2. Properties of the EPS geofoam materials [20]

EPS Type	Density (kg/m³)	Unit Weight (kN/m³)	Elastic modulus, E (kPa)	Poisson's ratio (ν)
EPS 22	21.6	0.22	7500	0.10
EPS 29	28.8	0.29	10500	0.10
EPS 39	38.4	0.39	15000	0.10

3-3- Retaining Wall

The retaining wall was modeled as a plate element in PLAXIS 2D. The wall was concrete, 5 m high and 0.38 m thick. Its equivalent plate properties are summarized in Table 3.

Table 3. Properties of the retaining wall

Property	Unit	Value
Material	–	Concrete
EA	kN/m	1.178×10^{7}
EI	kN·m²/m	1.418×10^{5}
Thickness, d	m	0.38
Weight	kN/m/m	9.5
ν	–	0.2

4- Numerical Modeling

The numerical analyses were performed using the finite-element software PLAXIS 2D, based on a two-dimensional plane-strain formulation, which is appropriate for retaining-wall systems that extend sufficiently in the out-of-plane direction and are subjected to approximately uniform conditions along the wall axis [22–24]. The retaining wall was simulated using a plate element in PLAXIS 2D. The plate properties were defined based on the actual geometric and mechanical characteristics of the reinforced concrete wall. The axial stiffness (EA) and bending stiffness (EI) were calculated from the elastic modulus and the cross-section properties of the concrete for the wall thickness of 0.38 m. The above-obtained parameters are summarized and used in the numerical model and shown in Table 3. The baseline soil profile consisted of a 5 m-thick layer of fine-grained clay behind the wall and a 2 m-thick layer of sand beneath the wall. Other soil configurations were also considered to study the effect of soil type and stratification on the response of the retaining-wall system.

The soil behavior was simulated using the Mohr–Coulomb constitutive model. Drained analyses were performed using the effective strength and stiffness parameters listed in Table 1. Undrained analyses were performed using the PLAXIS Undrained B formulation, in which effective stiffness parameters are combined with directly specified undrained shear strength. The concrete retaining wall and EPS geofoam were modeled as linear-elastic materials. The EPS geofoam was positioned as a vertical compressible inclusion adjacent to the back face of the retaining wall, allowing its low unit weight and compressibility to modify the transfer of lateral stress to the wall [25–27].

The retaining wall and its foundation were modeled using plate elements embedded within the soil domain; therefore, no separate prescribed support condition was imposed at the wall base. Interface elements were assigned along the wall–soil contact surfaces, with Rinter = 0.67 for the concrete wall–soil interface. For models incorporating EPS geofoam, interfaces were also introduced along the concrete wall–EPS and EPS–soil contacts, with Rinter = 0.60 adopted. In the absence of site-specific interface shear-test data, these values were adopted as representative interface-strength reduction factors.

Standard displacement boundary conditions were applied: the lateral boundaries were fixed in the horizontal direction and free in the vertical direction, whereas the bottom boundary was fixed in both directions. The ground surface remained unconstrained. The computational boundaries were located sufficiently far from the retaining system to minimize boundary effects.

The initial geostatic stress field was generated using the K_0 procedure. The retaining wall and foundation elements, along with their corresponding interfaces, were subsequently activated. For geofoam-containing models, the EPS inclusion and associated interfaces were activated in the corresponding construction phase. Excavation was simulated by deactivating the soil cluster in front of the wall. No external surcharge was applied; hence, the calculated lateral earth pressure and wall deformation resulted from the self-weight of the retained soil and excavation-induced stress redistribution. Fifteen-node triangular elements were employed for the finite-element discretization, with mesh refinement in the vicinity of the retaining wall, interfaces, and geofoam inclusion. The numerical model is presented in Figure 1.

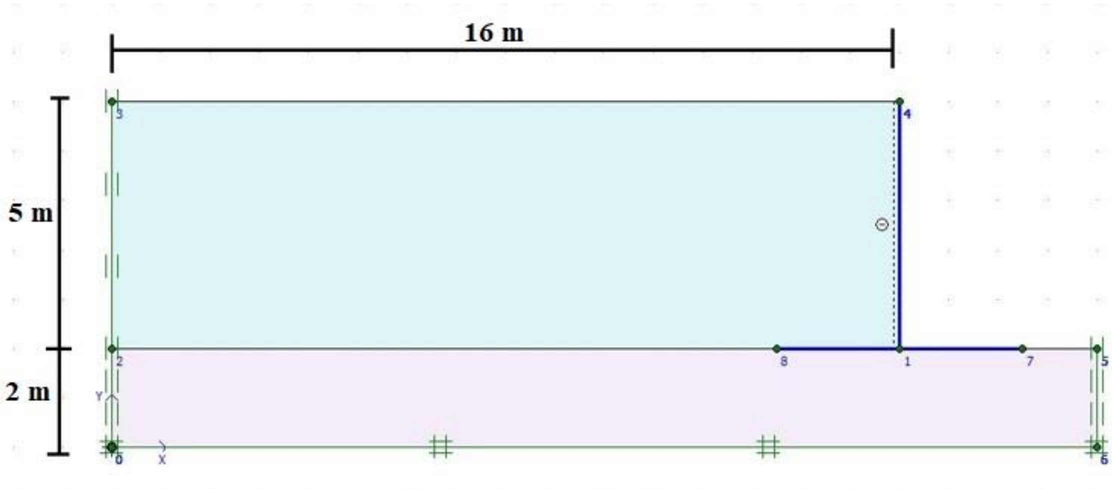

Figure 1. Baseline finite-element model of the retaining wall and soil profile.

The analyses were conducted under both drained and undrained static conditions. In the drained analyses, excess pore-water pressure was allowed to dissipate. For the undrained cases, the groundwater table was assumed at the ground surface, and the fine-grained soil layers were assigned the Undrained B drainage type in PLAXIS 2D. Undrained B performs an effective-stress analysis using effective stiffness parameters together with directly specified undrained strength. Accordingly, the Young's modulus and Poisson's ratio listed in Table 1 were retained as effective stiffness inputs, while the undrained shear strength was specified directly with ϕu = 0 and c = su. Excess pore-water pressure was generated during the undrained calculation, while the prescribed su controlled the available shear strength.

The undrained shear strengths adopted for the CL and ML layers were su = 17 kPa and su = 19 kPa, respectively, as summarized in Table 1. Because the SM layer represents a comparatively permeable granular soil, the undrained sensitivity analysis was principally relevant to the CL and ML fine-grained layers. The same geometry, structural properties, boundary conditions, interface parameters, and construction sequence were maintained between the drained and undrained cases. This definition makes the short-term analyses consistent with the PLAXIS Undrained B effective-stress formulation with prescribed undrained strength [24]. The importance of coupled pore-pressure and deformation response in numerical analyses of fine-grained soils has also been emphasized in recent finite-element studies [28].

The effect of the properties of EPS geofoam on retaining-wall response was evaluated for three EPS grades with unit weights of 0.22, 0.29 and 0.39 kN/m3 (densities of 21.6, 28.8 and 38.4 kg/m3, respectively) and four inclusion thicknesses of 0.5, 1.0, 1.5 and 2.0 m. The baseline model did not have any geofoam, whereas the other models had EPS placed behind the retaining wall. The investigated configurations and sensitivity analyses are summarized in Table 4.

5- Numerical Benchmark Comparison and Model Verification

Before conducting the parametric analyses, the numerical framework was checked against a documented numerical benchmark from the PLAXIS 2D Validation Manual [29]. Because the reference solution is numerical rather than independent experimental or field evidence, the procedure is described here as a numerical benchmark comparison and model verification, rather than experimental validation.

Table 4. Numerical cases considered in the study

Case	Description
Baseline	Upper clay layer and lower sand layer; effect of geofoam type and thickness.
1	Upper silt layer and lower sand layer; effect of geofoam type and thickness.
2	Entire backfill as fine-grained clay; effect of geofoam type and thickness.
3	Entire backfill as fine-grained silt; effect of geofoam type and thickness.
4	Entire backfill as loose silty sand; effect of geofoam type and thickness.
5	Undrained upper clay layer and lower sand layer; effect of geofoam.
6	Undrained upper silt layer and lower sand layer; effect of geofoam.
7	Effect of retaining-wall height and geofoam behavior.

For the selected benchmark, the reported geometry, material properties, constitutive assumptions, loading sequence, and boundary conditions were reproduced in PLAXIS 2D. The comparison focused on lateral wall displacement, which provides a direct measure of the deformation response of the modeled soil–wall system.

Figure 2 compares the lateral displacement obtained from the present PLAXIS model with the published benchmark response. The displacement profiles show close agreement along the wall height; the maximum difference was approximately 4 mm, corresponding to a relative difference of about 2%. This agreement supports the numerical consistency of the adopted model implementation for the benchmark configuration.

A mesh-sensitivity check was also carried out by refining the mesh around the retaining wall, interfaces, and EPS inclusion, where the largest stress and displacement gradients were expected. The final mesh was selected when further refinement produced only negligible changes in calculated lateral displacement and lateral earth pressure. On this basis, the numerical framework was considered suitable for the subsequent comparative parametric analyses.

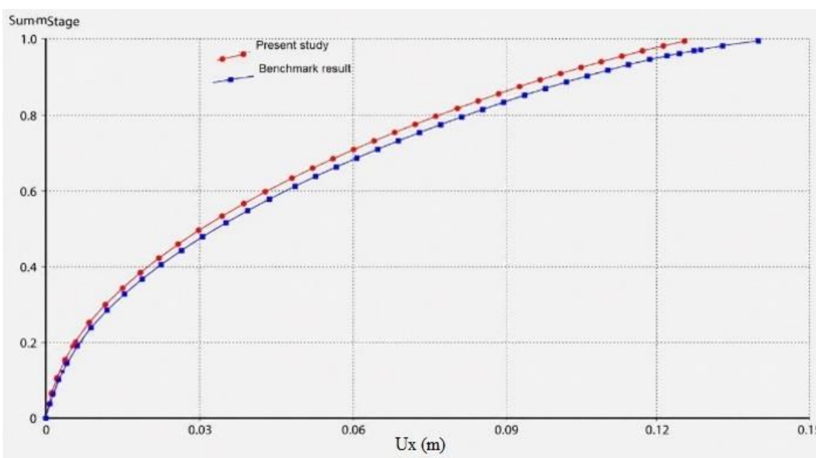

Figure 2. Numerical benchmark comparison of lateral wall displacement between the present PLAXIS model and the reference solution reported in the PLAXIS 2D Validation Manual [29].

https://doi.org/10.22034/cpj.2026.598896.1470

6-Results and Discussion

6-1- Selection of Geofoam Unit Weight and Thickness

The baseline model consisted of a 5 m clay backfill behind the retaining wall and a 2 m sand layer below the wall. The first configuration studied was the unreinforced case (Fig. 1). EPS-22, EPS-29, and EPS-39, with unit weights of 0.22, 0.29, and 0.39 kN/m³, respectively, were then added at thicknesses of 0.5, 1.0, 1.5, and 2.0 m (Fig. 3). Lateral earth pressure and wall displacement were evaluated as a function of EPS grade/unit weight and inclusion thickness.

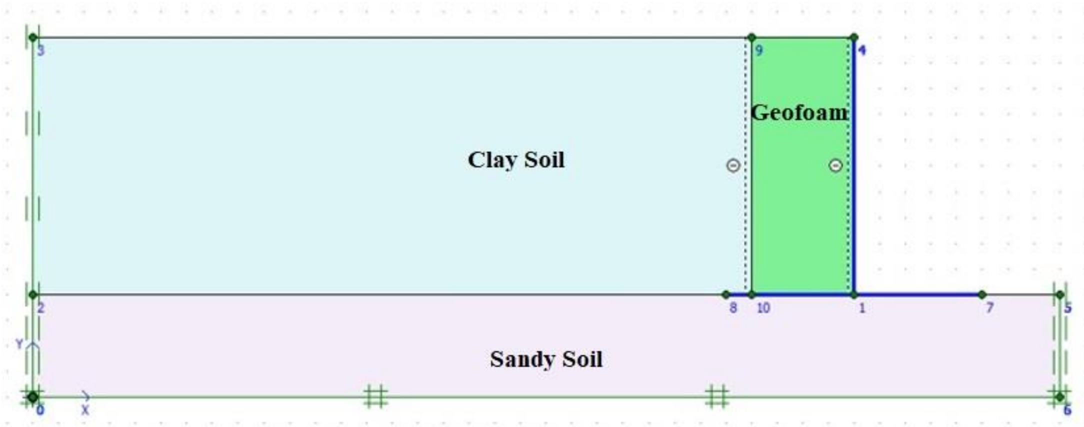

Figure 3. Finite-element model with EPS geofoam inclusion.

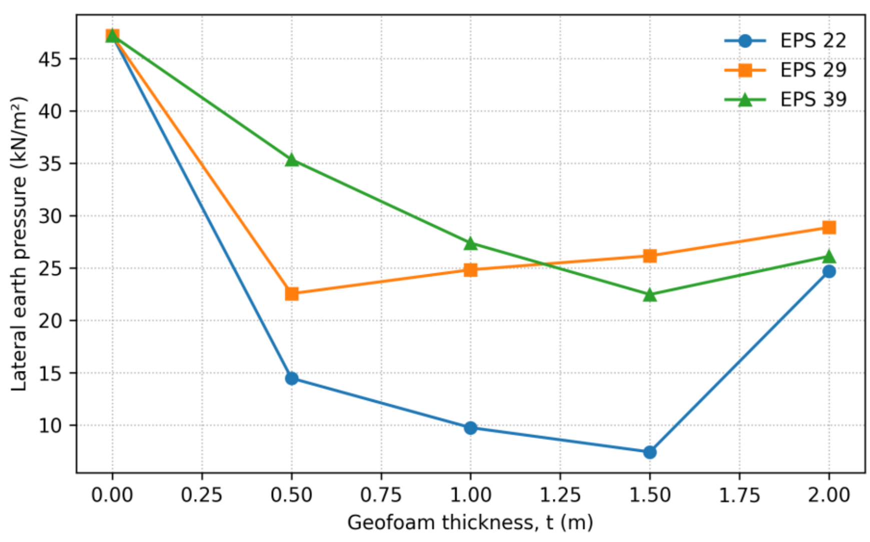

Figure 4. Effect of EPS geofoam unit weight and thickness on lateral earth pressure.

As shown in Figure 4, the largest stepwise reduction in lateral earth pressure generally occurred when the EPS thickness reached approximately 1.0 m. Beyond 1.0 m, the incremental response was smaller relative to the initial improvement and was non-monotonic for some EPS grades; therefore, thicker inclusions may still provide additional reduction in individual cases. Accordingly, 1.0 m was adopted as a practical reference thickness within the investigated range rather than as the outcome of a formal optimization. At this thickness, EPS-22, EPS-29, and EPS-39 reduced lateral earth pressure by approximately 79.3%, 48.6%, and 41.0%, respectively, relative to the unreinforced case. EPS-

22, which had the lowest unit weight and density among the investigated grades, produced the largest reduction at this reference thickness.

The stronger pressure-relief response of the lower-unit-weight EPS grade is associated with its greater compressibility and capacity to accommodate deformation behind the wall, thereby reducing stress transferred to the retaining structure. However, lower-density EPS should be checked against allowable compressive strain and long-term deformation requirements. The observed sensitivity to inclusion thickness is consistent with earlier numerical and experimental investigations of EPS compressible inclusions [11,30].

The presence of EPS also reduced the maximum lateral displacement of the retaining wall, as shown in Figure 5. For the investigated configurations, the maximum reductions in displacement were approximately 22.1%, 19.1%, and 14.6% for EPS-22, EPS-29, and EPS-39, respectively. Increasing the inclusion thickness to about 1.0 m produced a pronounced reduction, after which the incremental change generally diminished. This behavior is consistent with the greater deformability of the lower-unit-weight EPS grade. El-Kady et al. [31] likewise reported reduced wall deformation when geofoam blocks were installed behind retaining walls.

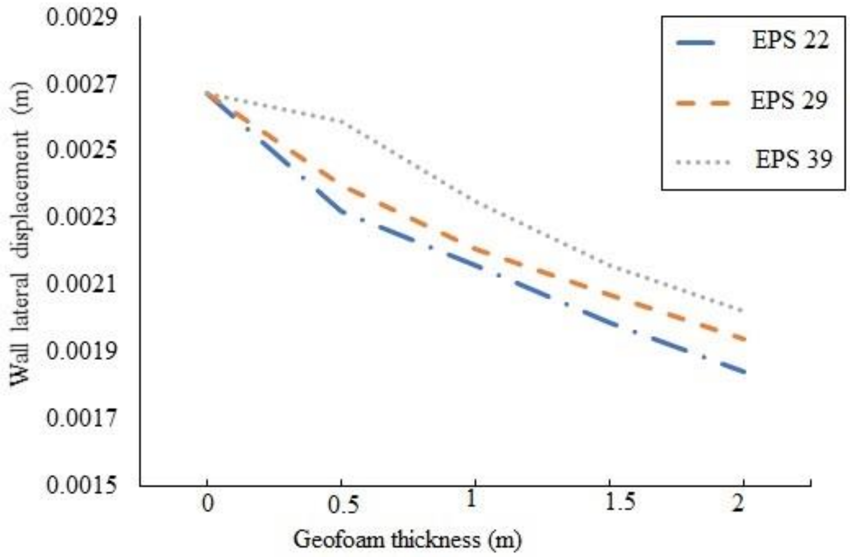

Figure 5. Effect of EPS geofoam unit weight and thickness on maximum lateral wall displacement.

6-2- Comparison of Numerical and Analytical Lateral Earth Pressure Distribution

To provide an analytical reference for the numerical results, the lateral earth-pressure distribution obtained from PLAXIS was compared with a conventional at-rest earth-pressure distribution. This comparison is used as a consistency check rather than as an exact analytical representation of the final post-excavation stress state. In the finite-element model, the initial geostatic stresses were generated using the K_0 procedure; subsequent excavation of the soil in front of the retaining wall allowed wall deformation and stress redistribution to develop. Therefore, the final numerical stress state is not assumed to remain strictly at rest.

For the analytical reference, the lateral effective stress at depth (z) was calculated as [32]:

$$\sigma_0 = \gamma z K_0 \quad (1)$$

and the corresponding resultant lateral force per unit length of wall was obtained from:

$$P_0 = \frac{1}{2} K_0 \gamma H^2 \quad (2)$$

where (K_0) is the coefficient of lateral earth pressure at rest, γ is the soil unit weight, z is the depth below the ground surface, and H is the wall height. For the fine-grained soil considered in the reference case, K0 was estimated from the adopted empirical relationship [32]:

$K_0 = 0.44 + 0.42(PI/100)$ (3)

where PI is the plasticity index of the soil.

For the CL soil used in the analytical reference comparison, the plasticity index was calculated from the Atterberg limits given in Table 1:

$PI=LL-PL=45-20=25$

Accordingly:

$K_0=0.44+0.42(25/100) =0.545$

Using the wet unit weight $\gamma wet = 17.1\ kN/m^3$ and wall height H = 5 m, the analytical lateral pressure at the base of the wall is:

$\sigma_0=17.1\times5\times0.545=46.6kPa$

Figure 6 presents the comparison between the analytical and numerical lateral earth-pressure distributions along the wall height. The corresponding PLAXIS value was 47.19 kPa, resulting in a difference of approximately 1.3% at the wall base. The close agreement at this depth indicates consistency in the order of magnitude of the calculated lateral stress. However, differences occur along the wall height because the analytical solution assumes a simplified at-rest stress distribution, whereas the finite-element model accounts for excavation-induced wall deformation, stress redistribution, soil–structure interaction, interface behavior, and the adopted constitutive representation of the soil. Accordingly, the analytical comparison should be regarded as a reference consistency check rather than a validation of the complete post-excavation numerical stress distribution.

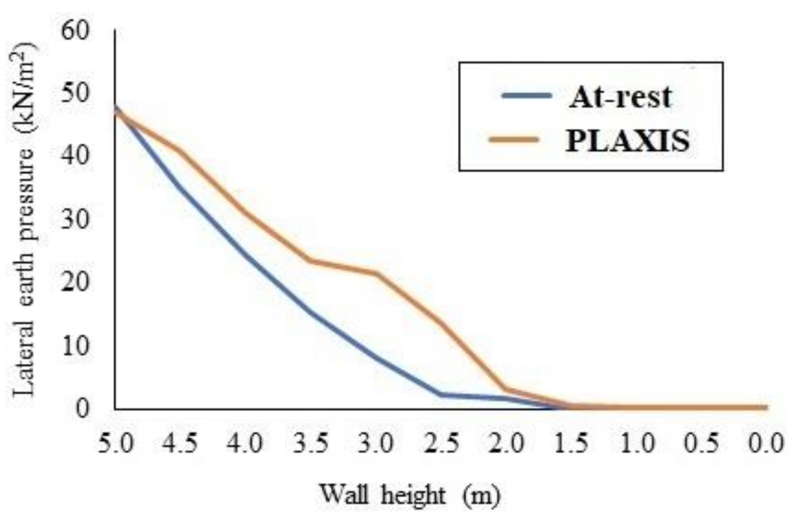

Figure 6. Comparison of the PLAXIS lateral earth-pressure distribution with the analytical at-rest earth-pressure reference.

Civil and Project Journal, 2027, 8(11), 42-58
https://doi.org/10.22034/cpj.2026.598896.1470

6-3- Sensitivity Analyses

6-3-1- Effect of Soil Type

The effect of the soil type was studied for the profiles of clay, silt, and sand, with a fixed height of the retaining wall equal to 5 m and a total height of the soil equal to 7 m. The reference configuration used in the practical application was the one identified in Section 6.1, i.e., EPS-22 (unit weight 0.22 kN/m3, density 21.6 kg/m3) with a thickness of 1.0 m. The use of geofoam reduced the lateral earth pressure by about 48.8%, 80.8%, and 46.3% in clay, silt, and sand, respectively. The maximum reduction was obtained with the ML soil, indicating that the efficiency of a compressible inclusion is very sensitive to the stiffness and strength characteristics of adjacent soils.

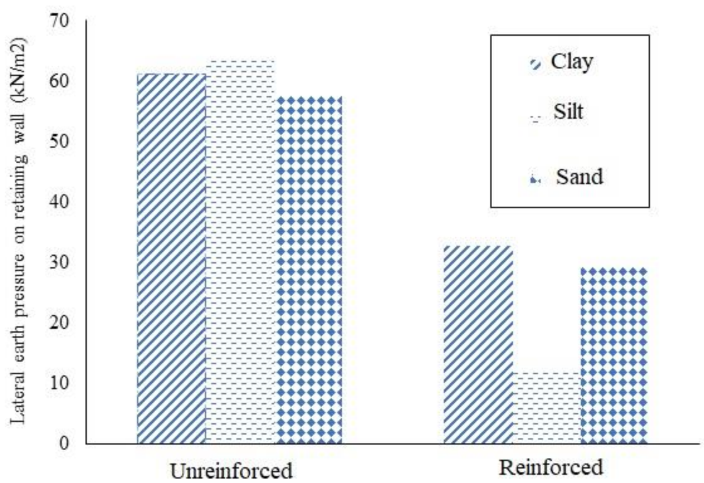

Figure 7. Effect of soil type on lateral earth pressure with and without geofoam.

Soil shear strength and stiffness influence the magnitude and redistribution of lateral earth pressure. Under comparable stress and deformation conditions, soils with greater frictional resistance generally mobilize lower lateral pressures, whereas low-strength fine-grained soils can impose higher lateral pressures. A compressible EPS layer adjacent to the wall accommodates part of the backfill deformation and modifies stress transfer to the wall. Similar sensitivity of geofoam performance to backfill and EPS properties has been reported in previous numerical studies [12,21].

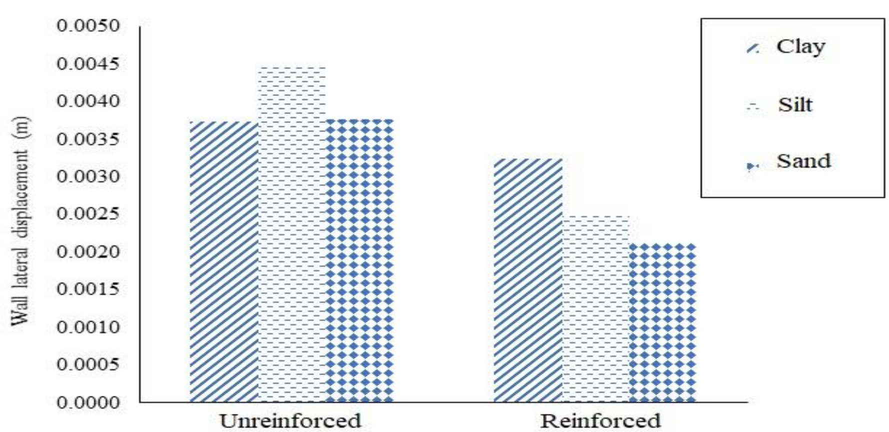

Figure 8. Effect of soil type on maximum lateral wall displacement with and without geofoam.

Civil and Project Journal, 2027, 8(11), 42-58
https://doi.org/10.22034/cpj.2026.598896.1470

The effect of soil type on the maximum lateral wall displacement, with and without geofoam, is shown in Figure 8. For all three soil types, geofoam reduced the wall displacement. The greatest reduction was for the ML soil. The reductions were of the order of 13.4% for clay, 44.0% for silt, and 43.2% for sand. The large reduction in displacement for the ML and SM profiles is in agreement with their low resistance to deformation and the improved ability of the geofoam layer to accommodate part of the backfill movement.

6-3-2- Effect of Soil Stratification

Three soil stratification patterns were investigated to examine the combined influence of soil layering and geofoam. The practical reference configuration, EPS-22 (unit weight 0.22 kN/m³; density 21.6 kg/m³) with a thickness of 1.0 m, was used in all cases. The investigated profiles are illustrated schematically in Figure 9.

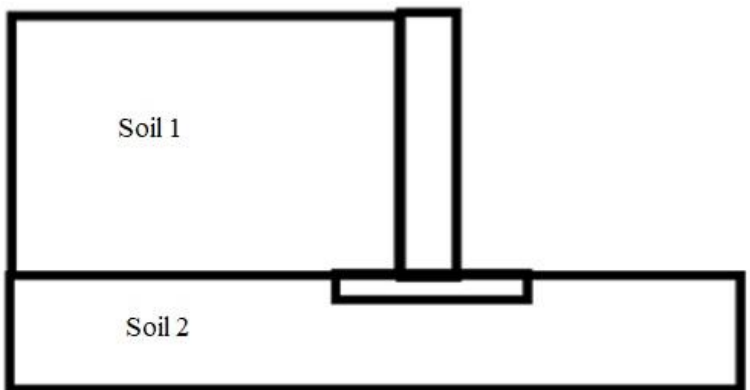

Case study	Soil 1	Soil 2
1	CL	SM
2	ML	SM
3	SM	CL

Figure 9. Soil stratification cases considered in the sensitivity analysis.

The effect of reinforcement on the lateral earth pressure acting on the retaining wall is shown in Figure 10 under the conditions presented. The maximum lateral pressure reduction was approximately 79.3% for the clay-over-sand profile, 78.2% for the silt-over-sand profile, and 47.75% for the sand-over-clay profile. The clay-over-sand configuration therefore exhibited the greatest benefit from geofoam. The differences among the profiles demonstrate that the response cannot be interpreted solely from average soil properties; the positions of weak and strong layers relative to the wall and foundation levels also affect stress redistribution. Fine-grained layers with low friction angle tend to generate greater lateral pressures, while the compressible geofoam layer reduces the portion of this load transferred directly to the wall.

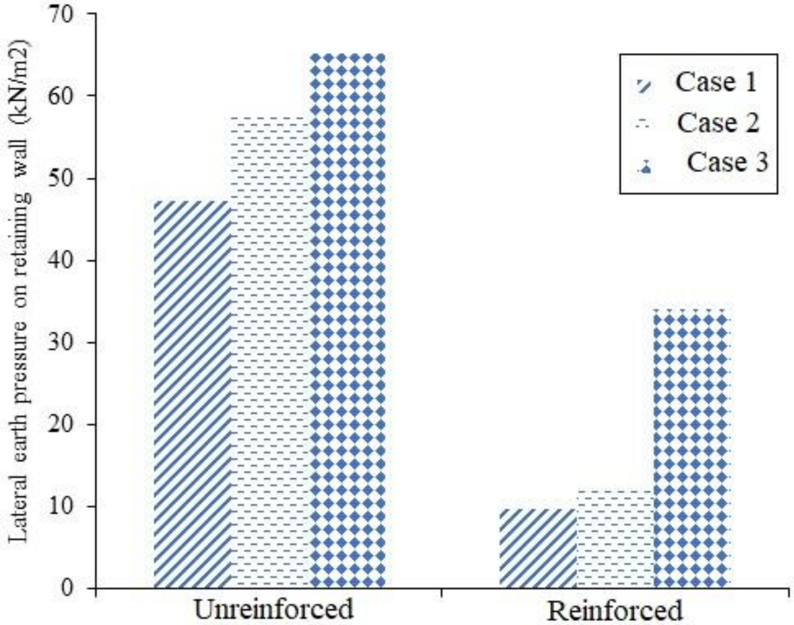

Figure 10. Effect of soil stratification on lateral earth pressure.

6-3-3- Effect of Retaining-Wall Height

The influence of wall height was investigated at 3, 5, 6, and 8 m. EPS-22 (unit weight 0.22 kN/m³; density 21.6 kg/m³) was used with a thickness-to-wall-height ratio of 0.2, consistent with the practical reference ratio adopted for the 5 m baseline wall. Increasing wall height increased the absolute lateral earth pressure because of the greater soil overburden and associated lateral stress demand.

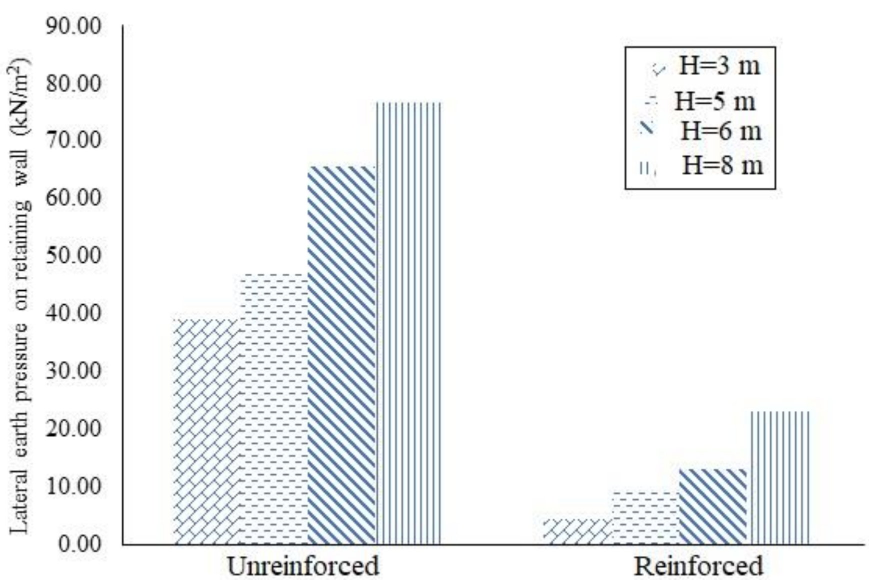

Figure 11. Effect of retaining-wall height on lateral earth-pressure reduction.

Figure 11 shows that increasing wall height increases the absolute lateral earth pressure. The calculated reductions were approximately 88.7%, 79.3%, 79.9%, and 70.0% for wall heights of 3, 5, 6, and 8 m, respectively. Although the trend is not strictly monotonic between 5 and 6 m, the 8 m wall shows a lower relative reduction than the shorter-wall cases. This result demonstrates that EPS thickness and grade should be selected in conjunction with wall height and the associated stress level rather than by adopting a universal configuration.

6-3-4- Effect of Drainage Condition

The effect of drainage was investigated by placing the groundwater table at the ground surface and analyzing the fine-grained soil cases using the Undrained B formulation described in Section 4. The practical reference EPS configuration (EPS-22 with unit weight 0.22 kN/m³ and 1.0 m thickness) was retained for comparison. The resulting pressure distributions are shown in Figure 12.

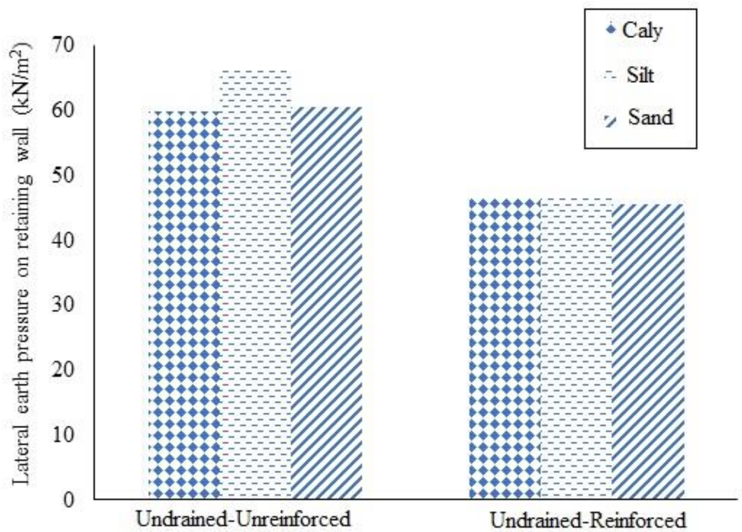

Figure 12. Changes in lateral earth pressure in undrained conditions.

Under the investigated undrained conditions, EPS reduced total lateral earth pressure by approximately 22–28%, substantially lower than the 50–80% reductions observed in the drained analyses. With the groundwater table at the ground surface, pore-water pressure contributes to total lateral stress, whereas the compressible EPS inclusion primarily modifies stress transfer through the soil skeleton. Consequently, the relative reduction in total lateral pressure is smaller under the undrained groundwater condition considered here. This result highlights the importance of drainage conditions when assessing EPS performance behind retaining structures.

7- Conclusions

The performance of EPS geofoam in reducing lateral earth pressure and wall displacement was evaluated using two-dimensional finite-element modeling in PLAXIS 2D. The baseline case comprised a 5 m-high concrete retaining wall, a 5 m clay backfill, and a 2 m sand layer beneath the wall. Three EPS grades with unit weights of 0.22, 0.29, and 0.39 kN/m³ (densities of 21.6, 28.8, and 38.4 kg/m³) and four inclusion thicknesses from 0.5 to 2.0 m were investigated.

- Within the investigated range, EPS-22 with a thickness of 1.0 m was adopted as a practical reference configuration. At this thickness, lateral earth pressure and maximum wall displacement for the baseline clay–sand profile were reduced by approximately 79% and 22%, respectively. Increasing thickness beyond 1.0 m produced smaller and non-monotonic incremental changes for some configurations; therefore, 1.0 m should be interpreted as a practical threshold for the present parametric study rather than as a formal optimization result.

- EPS performance was strongly dependent on soil type. Lateral earth-pressure reductions were approximately 48.8% in clay, 80.8% in silt, and 46.3% in sand for the corresponding sensitivity cases, demonstrating that the response of the compressible inclusion depends on the stiffness and strength characteristics of the surrounding soil.
- Soil stratification also affected the stress relief response. The clay-over-sand, silt-over-sand, and sand-over-clay profiles produced pressure reductions of approximately 79.3%, 78.2%, and 47.8%, respectively, indicating that the relative positions of weaker and stronger layers affect stress redistribution and should be considered when selecting EPS location and thickness.
- Wall height affected both the absolute lateral pressure and the relative performance of the adopted proportional EPS configuration. Pressure reductions of approximately 88.7%, 79.3%, 79.9%, and 70.0% were obtained for wall heights of 3, 5, 6, and 8 m, respectively, indicating that EPS dimensions and grade should be evaluated together with the stress level associated with wall height.
- Under the investigated undrained conditions, EPS reduced total lateral earth pressure by approximately 22–28%, compared with approximately 50–80% in the drained analyses. The smaller relative reduction is consistent with the contribution of pore-water pressure to total lateral stress when the groundwater table is at the ground surface.
- The analytical at-rest earth-pressure reference and the PLAXIS result agreed closely at the wall base (46.6 and 47.19 kPa, respectively), while larger differences occurred along the wall height. This comparison supports consistency in the stress magnitude at the base but also demonstrates that the post-excavation finite-element response includes wall deformation, stress redistribution, soil–structure interaction, and interface effects that are not represented by the simplified at-rest analytical distribution.
- Overall, the results indicate that EPS geofoam can provide an effective lightweight and compressible inclusion for reducing static lateral loads on retaining walls. Practical selection should consider EPS grade (density and unit weight), thickness, wall height, soil type and stratification, groundwater/drainage conditions, allowable deformation, and long-term compressive behavior rather than relying on a single universally applicable configuration.

Limitations and Future Research

The present study was based on two-dimensional finite-element analyses and the Mohr–Coulomb model; therefore, three-dimensional effects and advanced nonlinear soil behavior were not considered. In addition, EPS geofoam was modeled as a linear-elastic material, while its nonlinear compressive response and long-term creep behavior require further investigation. Future work should consider three-dimensional geometry, improved constitutive models for soil and EPS, and coupled hydro-mechanical conditions with variable groundwater level. It is also recommended to conduct experimental and field-scale studies under cyclic and seismic loading to validate and extend the present numerical results.

Conflict of Interest

The authors declare that they have no financial, institutional, professional, or personal conflicts of interest related to this study.

Declaration on the Use of Artificial Intelligence

Generative artificial intelligence tools were used solely to assist with language editing and grammatical refinement. These tools were not used for data generation, numerical modeling, PLAXIS analyses, result calculations, or scientific interpretation. All AI-assisted edits were critically reviewed and thoroughly verified by the authors, who retain full responsibility for the accuracy, integrity, and scientific content of the manuscript.

Funding

This research received no specific grant or financial support from any public, commercial, or not-for-profit funding agency.

References

1. Horvath, J. S. (2008). Seismic lateral earth pressure reduction on earth-retaining structures using geofoams. In Geotechnical Earthquake Engineering and Soil Dynamics IV (pp. 1–10). American Society of Civil Engineers. https://doi.org/10.1061/40975(318)155
2. Hajian, M., & Attarnejad, R. (2022). Non-uniform relationship for soil-foundation reaction. Civil and Project Journal, 4(5), 11–20. https://doi.org/10.22034/CPJ.2022.349082.1145
3. Ghavami, S., Hallaji, A., & Sandooghsaz, Y. (2025). Assessment of the effect of fly ash and nanosilica on the geotechnical properties of forest road subgrade. Civil and Project Journal, 7(5), 73–88. https://doi.org/10.22034/CPJ.2025.527515.1373
4. Sanders, R. L. (1996). United Kingdom design and construction experience with EPS. In Proceedings of the International Symposium on EPS (Expanded Polystyrol) Construction Method (EPS Tokyo '96) (pp. 235–246). Tokyo, Japan.
5. Zarnani, S., & Bathurst, R. J. (2009). Numerical parametric study of expanded polystyrene (EPS) geofoam seismic buffers. Canadian Geotechnical Journal, 46(3), 318–338. https://doi.org/10.1139/T08-128
6. Ertugrul, O. L., & Trandafir, A. C. (2013). Lateral earth pressures on flexible cantilever retaining walls with deformable geofoam inclusions. Engineering Geology, 158, 23–33. https://doi.org/10.1016/j.enggeo.2013.03.001
7. Chauhan, V. B., & Dasaka, S. M. (2017). Assessment of lateral earth pressure reduction using EPS geofoam—A numerical study. In Proceedings of the Conference on Numerical Modeling in Geomechanics (CoNMiG-2017), IIT Roorkee, India, 3–4 March 2017 (Paper ID 01, pp. 1–8).
8. Hasanpouri Notash, N., & Dabiri, R. (2018). Effects of geofoam panels on static behavior of cantilever retaining wall. Advances in Civil Engineering, 2018, Article 2942689. https://doi.org/10.1155/2018/2942689
9. Dabiri, R., & Hasanpouri Notash, N. (2020). Evaluation of geofoam effects on seismic response in cantilever retaining wall. Geotechnical and Geological Engineering, 38(2), 2097–2116. https://doi.org/10.1007/s10706-019-01151-1

10. Xie, M., Zheng, J., Shao, A., Miao, C., & Zhang, J. (2020). Study of lateral earth pressures on nonyielding retaining walls with deformable geofoam inclusions. Geotextiles and Geomembranes, 48(5), 684–690. https://doi.org/10.1016/j.geotexmem.2020.05.003
11. Gade, V. K., & Dasaka, S. M. (2022). Short- and long-term behavior of EPS geofoam in reduction of lateral earth pressure on rigid retaining wall subjected to surcharge loading. Geotextiles and Geomembranes, 50(5), 868–880. https://doi.org/10.1016/j.geotexmem.2022.05.002
12. Han, Z., Zou, W.-L., Ying, Z.-Q., Feng, H.-P., & Yang, G.-Q. (2023). A semi-empirical approach for estimating the lateral earth pressure on rigid retaining walls with EPS inclusions in cohesionless soils. Transportation Geotechnics, 39, 100937. https://doi.org/10.1016/j.trgeo.2023.100937
13. Fan, K., Yang, G., Zou, W., Han, Z., & Shen, Y. (2024). Lateral earth pressure of granular backfills on retaining walls with expanded polystyrene geofoam inclusions under limited surcharge loading. Journal of Rock Mechanics and Geotechnical Engineering, 16(4), 1388–1397. https://doi.org/10.1016/j.jrmge.2023.11.005
14. Sheeley, M. (2000). Slope stabilization utilizing geofoam. MS Thesis, Syracuse University.
15. Beju, Y. Z., & Mandal, J. N. (2017). Expanded polystyrene (EPS) geofoam: Preliminary characteristic evaluation. Procedia Engineering, 189, 239–246. https://doi.org/10.1016/j.proeng.2017.05.038
16. Khan, M. I., & Meguid, M. A. (2018). Experimental investigation of the shear behavior of EPS geofoam. International Journal of Geosynthetics and Ground Engineering, 4, Article 12. https://doi.org/10.1007/s40891-018-0129-7
17. Padade, A. H., & Mandal, J. N. (2012). Behavior of expanded polystyrene (EPS) geofoam under triaxial loading conditions. Electronic Journal of Geotechnical Engineering, 17, 2543–2553.
18. Beju, Y. Z., & Mandal, J. N. (2016). Compression creep test on expanded polystyrene (EPS) geofoam. International Journal of Geotechnical Engineering, 10(4), 401–408. https://doi.org/10.1080/19386362.2016.1155260
19. Yadav, P., Singh, D. K., Dahale, P. P., & Padade, A. H. (2020). Analysis of retaining wall in static and seismic condition with inclusion of geofoam using PLAXIS 2D. In Geohazards: Proceedings of IGC 2018 (pp. 223–240). Springer.
20. Khan, M. I., & Meguid, M. A. (2021). A numerical study on the role of EPS geofoam in reducing earth pressure on retaining structures under dynamic loading. International Journal of Geosynthetics and Ground Engineering, 7, Article 57. https://doi.org/10.1007/s40891-021-00304-8
21. Khan, M. I., & Meguid, M. A. (2021). Evaluating the role of geofoam properties in reducing lateral loads on retaining walls: A numerical study. Sustainability, 13(9), 4754. https://doi.org/10.3390/su13094754
22. Zdravković, L. (1999). Finite element analysis in geotechnical engineering: theory. Thomas Telford.
23. Potts, D. M., Zdravković, L., Addenbrooke, T. I., Higgins, K. G., & Kovačević, N. (2001). Finite element analysis in geotechnical engineering: application (Vol. 2, p. 427). London: Thomas Telford.

24. PLAXIS B.V. (2018). PLAXIS 2D Reference Manual. Delft, The Netherlands: PLAXIS B.V.
25. Horvath, J.S. (1995). Geofoam geosynthetic. Horvath Engineering, Scarsdale, New York, USA.
26. Stark, T. D., Arellano, D., Horvath, J. S., & Leshchinsky, D. (2004). Geofoam applications in the design and construction of highway embankments. NCHRP Web Document 65 (Project 24-11). Transportation Research Board, National Research Council, Washington, DC.
27. Duškov, M. (1997). Materials research on EPS20 and EPS15 under representative conditions in pavement structures. Geotextiles and Geomembranes, 15(1–3), 147–181. https://doi.org/10.1016/S0266-1144(97)00011-3
28. Pardsouie, M. M., Mokhberi, M., Zomorodian, S. M. A., & Pardsouie, M. H. (2023). Coupling effect and superposition law in soil treatment systems incorporating vacuum preloading. Civil and Project Journal, 5(4), 58–72. https://doi.org/10.22034/CPJ.2023.405822.1214
29. Brinkgreve, R. B. J., Broere, W., & Waterman, D. (2008). PLAXIS 2D Validation Manual, Version 9.0. Delft, The Netherlands: PLAXIS B.V.
30. Azzam, S. A., & AbdelSalam, S. S. (2015). EPS geofoam to reduce lateral earth pressure on rigid walls. In Proceedings of the International Conference on Advances in Structural and Geotechnical Engineering (ICASGE’15), Hurghada, Egypt.
31. El-Kady, M. S., Alzara, M. A., & Farouk, M. A. (2018). Reduction of lateral earth pressure using geo-foam blocks. Innovative Infrastructure Solutions, 3, Article 40. https://doi.org/10.1007/s41062-018-0145-4
32. Das, B. M., & Sivakugan, N. (2018). Principles of Foundation Engineering (9th ed.). Cengage Learning.